Stem Cell Research 17 (2016) 6–15

Contents lists available at ScienceDirect

Stem Cell Research

journal homepage: www.elsevier.com/locate/scr

# Development of a new therapeutic technique to direct stem cells to the infarcted heart using targeted microbubbles: StemBells

L. Woudstra [a,f], P.A.J. Krijnen [a,f], S.J.P. Bogaards [c,f], E. Meinster [a], R.W. Emmens [a,f], T.J.A. Kokhuis [g,h], I.A.E. Bollen [a,f], H. Baltzer [a], S.M.T. Baart [c], R. Parbhudayal [a], M.N. Helder [d], V.W.M. van Hinsbergh [c,f], R.J.P. Musters [c,f], N. de Jong [g,h,i], O. Kamp [e,f,g], H.W.M. Niessen [a,b,f], A. van Dijk [a,f], L.J.M. Juffermans [e,f,g,*]

[a] Department of Pathology, VU University Medical Center, Amsterdam, The Netherlands
[b] Department of Cardiac Surgery, VU University Medical Center, Amsterdam, The Netherlands
[c] Department of Physiology, VU University Medical Center, Amsterdam, The Netherlands
[d] Department of Orthopedics, VU University Medical Center, Amsterdam, The Netherlands
[e] Department of Cardiology, VU University Medical Center, Amsterdam, The Netherlands
[f] Institute of Cardiovascular Research (ICaR-VU), VU University Medical Center, Amsterdam, The Netherlands
[g] Interuniversity Cardiology Institute of the Netherlands (ICIN), Utrecht, The Netherlands
[h] Department of Biomedical Engineering, Erasmus MC, Rotterdam, The Netherlands
[i] Department of Acoustical Wavefield Imaging, Technical University of Delft, Delft, The Netherlands

ARTICLE INFO

*Article history:*
Received 15 March 2016
Received in revised form 21 April 2016
Accepted 28 April 2016
Available online 30 April 2016

*Keywords:*
Acute myocardial infarction
Adipose tissue-derived stem cells
Targeting
Microbubbles
StemBells
Acoustic radiation force

ABSTRACT

Successful stem cell therapy after acute myocardial infarction (AMI) is hindered by lack of engraftment of sufficient stem cells at the site of injury. We designed a novel technique to overcome this problem by assembling stem cell-microbubble complexes, named 'StemBells'.

StemBells were assembled through binding of dual-targeted microbubbles (~3 μm) to adipose-derived stem cells (ASCs) *via* a CD90 antibody. StemBells were targeted to the infarct area *via* an ICAM-1 antibody on the microbubbles. StemBells were characterized microscopically and by flow cytometry. The effect of ultrasound on directing StemBells towards the vessel wall was demonstrated in an *in vitro* flow model. In a rat AMI-reperfusion model, StemBells or ASCs were injected one week post-infarction. A pilot study demonstrated feasibility of intravenous StemBell injection, resulting in localization in ICAM-1-positive infarct area three hours post-injection. In a functional study five weeks after injection of StemBells cardiac function was significantly improved compared with controls, as monitored by 2D-echocardiography. This functional improvement neither coincided with a reduction in infarct size as determined by histochemical analysis, nor with a change in anti- and pro-inflammatory macrophages.

In conclusion, the StemBell technique is a novel and feasible method, able to improve cardiac function post-AMI in rats.



## 1. Introduction

Adult mesenchymal stem cell therapy has been proposed as a promising therapy for regenerative tissue repair, for example to prevent heart failure development after acute myocardial infarction (AMI) (Shah and Shalia, 2011; Wollert et al., 2004). However, one of the major problems of stem cell therapy is a lack of engraftment of sufficient stem cells at the site of injury (van Dijk et al., 2011; Berardi et al., 2011). We hypothesized that when retention and engraftment of stem cells are increased, the therapeutic effect of stem cells will improve. Therefore, we designed a novel targeting technique to direct adipose-derived stromal/stem cells (ASCs) specifically to the activated endothelium of blood vessels within the infarct area in the heart by coating them with dual-targeted microbubbles.

We used ASCs, because adipose tissue is a rich source of mesenchymal stem cells, which can be harvested easily, show high proliferation rates in culture and have the capacity to differentiate into several cell types amongst which cardiomyocytes (Oedayrajsingh-Varma et al., 2006; van Dijk et al., 2008; Carvalho et al., 2013; Rangappa et al., 2003). Furthermore, it has been shown that ASCs have a beneficial effect on cardiac function post-AMI in several pre-clinical studies (van Dijk et al., 2011; Berardi et al., 2011; Yamada et al., 2006). Early clinical trials

* Corresponding author at: VU University Medical Center, Department of Cardiology, De Boelelaan 1117, rm 4C099, 1081 HV Amsterdam, The Netherlands.
*E-mail address:* ljm.juffermans@vumc.nl (L.J.M. Juffermans).

http://dx.doi.org/10.1016/j.scr.2016.04.018

using ASC therapy post-AMI, however, show that there is a room for improvement for ASC therapy (Houtgraaf et al., 2012; Janssens et al., 2006; Jeevanantham et al., 2012; Assmus et al., 2014).

To be able to direct the ASCs to the infarct area we employed the so-called microbubbles, which are small (2–4 μm) gas-filled bubbles originally developed as contrast agents for echocardiography (Dijkmans et al., 2004). Nowadays, microbubbles can also be designed as targeting agents by conjugating antibodies, ligands or peptides to the microbubble shell (Klibanov et al., 2004; Kokhuis et al., 2013). We have constructed stem cell-microbubble complexes, named 'StemBells', by coating ASCs with microbubbles using a CD90 antibody *via* biotin-streptavidin bridging (Fig. 1A). Additionally, an antibody against ICAM-1, an adhesion molecule expressed on activated endothelium of blood vessels within the infarct area (Benson et al., 2007), was simultaneously conjugated to the microbubble shell to create a bridge and improve the attachment of the StemBells specifically in the infarct area. Application of the microbubbles has several benefits. First, it allows coupling of a targeting antibody to the ASCs without modifying the stem cell itself. Second, the microbubbles cause buoyancy and susceptibility of the ASCs to the acoustic radiation force exerted by diagnostic ultrasound, as we previously showed in an chicken embryo using intravital microscopy (Kokhuis et al., 2014). StemBells can thus be pushed from the center of the blood stream to the vessel wall by ultrasound, further enhancing the effect of targeting.

Here, we describe the development and validation of this novel StemBell technique. We demonstrate its safety, as well as its positive effect on cardiac function in a rat AMI study.

## 2. Methods

### *2.1. Isolation and culture of the stromal vascular fraction from human and rat adipose tissue*

For isolation of the human stromal vascular fraction (SVF), subcutaneous abdominal adipose tissue samples were obtained as waste material after elective surgery and donated upon informed consent of the patients from three clinics in the Netherlands (Tergooi Ziekenuis, Hilversum; 'Jan van Goyen' clinic, Amsterdam; VU University Medical Center, Amsterdam). This study complied with the principles of the Declaration of Helsinki. SVF was isolated as described previously (Oedayrajsingh-Varma et al., 2006). Adipose tissue was stored in sterile phosphate-buffered saline (PBS; Braun, Melsungen, AG, USA) at 4 °C and processed within 24 h after surgery as described previously (Oedayrajsingh-Varma et al., 2006). In brief, adipose tissue was enzymatically digested using 0.1% collagenase A (Roche Diagnostics GmbH, Mannheim, Germany) in PBS containing 1% bovine serum albumin (BSA; Roche Diagnostics) for 45 min at 37 °C under intermittent shaking. To remove contaminating erythrocytes, the cells were subjected to Ficoll density centrifugation (Lymphoprep, ρ01.077 g/ml, osmolarity 280 ± 15 mOsm; Axis-Shield, Oslo, Norway).

For rat SVF isolation, adipose tissue from the inguinal fat pad of 30 male Wistar rats (Harlan Laboratories, Horst, the Netherlands; 300–400 g) was resected, pooled per 5 rats, collected in sterile PBS and processed immediately after resection as described previously (van Dijk et al., 2011). Animals were treated according to national guidelines and with permission of the Institutional Animal Care and local Animal

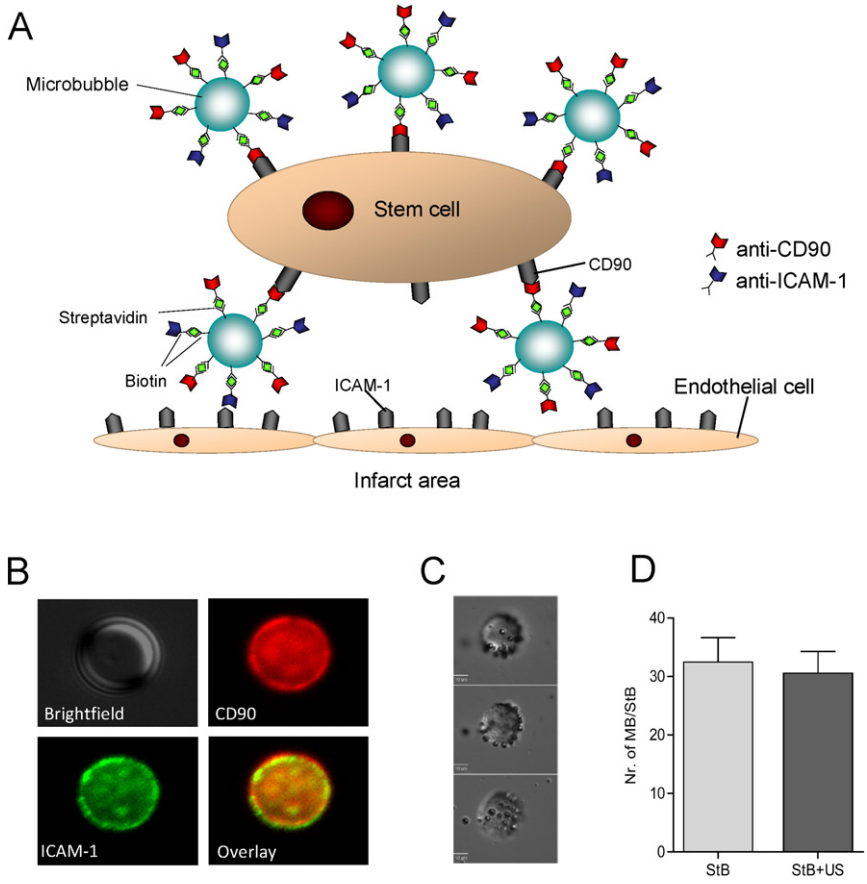


**Fig. 1.** StemBells A) Schematic drawing of a StemBell: a stem cell-microbubble complex coupled *via* streptavidin-biotin-antibody bridging. B) Microscopic images demonstrating the presence of two antibodies on one microbubble. Upper left panel: bright field image; upper right panel: anti-CD90 in red; lower left panel: anti-ICAM-1 in green, and lower right panel is an overlay. C) Microscopic bright field images showing three planes of a 3D stack of a StemBell. D) Quantification of the number of microbubbles per stem cell includes the effect of ultrasound. Data is shown as mean ± SEM (n = 6).

Ethical Committee of the VU University Medical Center (Amsterdam, the Netherlands), which conforms with the National Institutes of Health Guide for the Care and Use of Laboratory Animals (NIH Pub. No. 85-23, Revised 1996).

Both human and rat SVF cells were seeded at $1 \times 10^5$ cells/cm$^2$ in Dulbecco's modified Eagle's medium (DMEM; BioWhittaker, Cambrex, Verviers, Belgium) containing 100 U/ml penicillin, 100 μg/ml streptomycin, and 2 mM L-glutamine (all from Gibco, Invitrogen, Carlsbad, CA, USA). Culture medium for rat SVF cells was supplemented with 10% fetal bovine serum (FBS; HyClone, South Logan, UT, USA). For human SVF cells, culture medium was supplemented with 5% human platelet lysate and 10 IU/ml heparin (Leo Pharma, Amsterdam, the Netherlands) (Naaijkens et al., 2012). Cells were cultured in a humidified atmosphere of 5% $CO_2$ at 37 °C. Media were changed twice a week.

The percentage of ASCs within the SVF was determined by a colony forming unit assay. SVF cells were seeded in 6-well culture dishes (Greiner Bio one, USA) at a density of 10 and 100 cells/cm$^2$ (in triplicate) in ASC growth medium which consisted of low glucose Dulbecco's modified Eagle's medium (DMEM). After 14 days, cells were washed with PBS, fixed with 4% formalin for 10 min, and subsequently stained in a 1% toluidine blue solution in borax buffer for 1 min and washed twice with $H_2O$. Colonies containing at least 50 cells were scored using a Stereomicroscope (Zeiss, Germany).

Prior to *in vitro* experiments or *in vivo* injection SVF from liquid nitrogen storage was thawed and seeded at $1 \times 10^5$ cell/cm$^2$ in ASC growth medium. When ASCs reached 90% confluency, cells were detached with 0.5 mM EDTA/0.05% trypsin (Gibco). Cell size was determined using a Scepter handheld automatic cell counter (Millipore, Billerica, MA, USA). For *in vitro* experiments ASCs in passage 1 or 2 were used, for *in vivo* experiments ASCs were used in passage 1, and cultured for six days.

### 2.2. StemBell assembly

Biotinylated microbubbles with a perfluorobutane ($C_4F_{10}$) gas core were made by sonification, as described by Klibanov (Klibanov et al., 2004). The shell was composed of 1,2-distearoyl-*sn*-glycerol-3-phosphocholine (DSPC; 59.4 mol%; Sigma-Aldrich, the Netherlands); polyethylene glycol (PEG)-40 stearate (35.7 mol%; Sigma-Aldrich); 1,2-distearoyl-*sn*-glycerol-3-phosphoethanolamine (DSPE)-PEG(2000) (4.1 mol%; Avanti Polar Lipids) and DSPE-PEG(2000)-biotin (0.8 mol%; Avanti Polar Lipids). Microbubbles ($10^9$ per ml) had an average diameter of 3.5 μm and were stored in sealed glass vials with a $C_4F_{10}$ gas headspace to prevent deflation. To make dual-targeted microbubbles, 100 μl biotinylated microbubbles were washed twice with PBS/$C_4F_{10}$ by centrifugation (400*g*, 1 min, 4 °C) to remove superfluous biotin and resolved in PBS/$C_4F_{10}$. Next, streptavidin (1 mg/ml; Sigma) was added and the mixture was incubated at 4 °C for 25 min. Microbubbles were again washed to remove superfluous streptavidin and resolved in PBS/$C_4F_{10}$. Next, biotinylated mouse-anti-rat-CD90 (1 μg; BD Bioscience) and biotinylated mouse-anti-rat-ICAM-1 (1 μg; ACRIS) were added and the mixture was incubated at 4 °C for 25 min. These dual-targeted microbubbles were again washed and resolved in DMEM. Final concentration of the microbubbles was determined using a Multisizer 3 Coulter Counter (Beckman Coulter, Fullerton, CA, USA). The presence of both antibodies was verified using a Cy3-labeled anti-IgG1-mouse (Invitrogen) and a FITC-labeled anti-IgG2a-mouse (Invitrogen) by fluorescence microscopy (Marianas, I.I.I., Denver, CO, USA) with a 40× objective (Zeiss, Germany).

Prior to incubation with the dual-targeted microbubbles, ASCs were labeled with Hoechst 33342 (10 μg/ml; Invitrogen) at 37 °C for 30 min. *In vitro* testing demonstrated that this concentration provided adequate labeling up to 42 days, as determined by fluorescence microscopy. In addition, this concentration had no effect on cell viability, determined by the addition of propidium iodide (PI) to the cells and counting of PI-positive, *i.e.* dead cells. Hoechst labeling also had no effect on cell proliferation as determined by cell proliferation assay (data not shown). Hoechst-labeled ASCs were then incubated with dual-targeted microbubbles in a 100:1 ratio under continuous rotation at room temperature for 25 min. A minimum of 10 StemBells per preparation was analyzed for the number of microbubbles per StemBell, using differential interference contrast microscopy (Marianas) with a 40× objective providing 3D-images of a StemBell.

### 2.3. Ultrasound application protocol

Ultrasound was applied using a 1-MHz unfocused transducer (V303-SU, Panametrics Inc, Waltham, MA, USA) or a 500 kHz PZT transducer (V318, Panametrics Inc) coupled to an arbitrary waveform generator (33220A, Agilent, Palto Alto, CA, USA) and a linear 60-dB power amplifier (150A100B, Amplifier Research, Bothell, WA, USA). The ultrasound signal was monitored by a synchronized digital oscilloscope (GOULD DSO 465, Valley View, OH, USA). Peak negative acoustic pressure was 100 kPa as verified with a calibrated hydrophone (PA076; Precision Acoustics, Dorchester, UK). ASCs or StemBells in suspension were exposed to sine-wave ultrasound bursts with a 10% duty cycle and 1 kHz pulse repetition frequency for one minute. Rats were exposed to the same ultrasound protocol by positioning the transducer parasternal at the anterior wall and location of the infarct area.

### 2.4. Cell viability assay

Cell viability was analyzed by flow cytometry using an Annexin-V-FITC and Propidium Iodide (PI) Apoptosis Detection Kit (eBioscience, San Diego, USA), as described by the manufacturer, to test whether the assembly of StemBells, as well as the application of ultrasound affected cell viability. In short, following StemBell formation with or without ultrasound treatment, cells were labeled with Annexin-V in the dark for 30 min. Prior to analysis, PI was added for at least 30 s. Fluorescence of both Annexin-V and PI was measured with a FACS Calibur flow cytometer (BD Biosciences). Stem cells negative for both Annexin-V and PI were scored as viable. Data was analyzed with CellQuest-Pro software (BD Biosciences).

### 2.5. Attachment assay

To investigate the ability to attach to a surface despite the numerous microbubbles bound to the cell surface $48 \times 10^3$ StemBells with and without exposure to ultrasound were seeded in a culture dish. After seeding, cells were allowed to attach in a humidified incubator for 5, 10, or 20 min, followed by removing unattached cells by washing with PBS. The number of attached cells was quantified using CyQuant Cell Proliferation Kit (Invitrogen) according to the manufacturer's protocol.

### 2.6. In vitro flow system to assess acoustic radiation force

A VI-slide flow chamber (Ibidi, Martinsried, Germany) was mounted on the Marianas microscope allowing real-time visualization of acoustic radiation force acting on flowing StemBells. Shear stress on the StemBells ($1 \times 10^6$ cells/50 ml) was 0.2 dyn/cm$^2$. Sequel bright field images were made at 20 Hz. After 2 s the ultrasound was switched on for the total duration of the image capture, *i.e.* 20 s.

### 2.7. Rat model of acute myocardial infarction

An acute myocardial infarction was induced as described previously (van Dijk et al., 2011; van Dijk et al., 2009) in eight-week old male Wistar rats (300–400 g, Harlan, the Netherlands) that were housed under constant temperature (21–22 °C), humidity (60–65%) and light–dark periodicity (L:D 12:12). Experimental procedures started after two weeks of acclimatization. Rats were anesthetized using subcutaneous hypnorm/dormicum (fentanyl and fluanisone 0.5 ml/kg,

midazolam 5 mg/kg) injection, and were ventilated at 75 breaths/min, 10–0.4 mbar (Zoovent ventilator, Netherlands). Heart rate was monitored using Einthoven I ECG. A left thoracotomy in the fourth intercostal space was made, and the left anterior descending coronary artery was ligated using a 6.0 prolene suture (Ethicon, Germany). Ischemia was maintained for 40 min, followed by reperfusion and chest closure. This procedure results in relatively small non-aneurysmatic infarcts, comparable to what occurs in the majority of patients suffering from AMI (Pfeffer et al., 1979). StemBells or ASCs (both $1 \times 10^6$/600 μl DMEM) or vehicle (an equal volume of DMEM alone) were injected intravenously (i.v.) in the tail vein one week post-AMI under isoflurane (3%) anesthesia. Directly prior to injection the suspension was vigorously resuspended to prevent clustering of the ASCs or StemBells.

A pilot short-term experiment was carried out in five rats to test whether ICAM-1 targeted StemBells (~20 μm ∅) injected intravenously were able to bind in the infarcted myocardium and whether they co-localized with ICAM-1 positivity in the infarct area three hours post-injection.

In the long-term functional experiment 27 rats were anesthetized one week post-AMI and injected with either ASCs (n = 11), StB (n = 9) or Vehicle (n = 7), followed by ultrasound exposure. Animals were sacrificed five weeks post-injection and putative effects on stem cell retrieval and differentiation, cardiac function, infarct size and macrophage infiltration were analyzed. For analysis of cardiac function, 2D-echocardiograpy was performed prior to AMI (baseline), prior to injection (day 7) and prior to sacrifice (day 42), using a 13 MHz linear-array transducer (ProSound SSD-4000 PureHD, Aloka, Tokyo, Japan). Short-axis images were analyzed to determine wall thickness and lumen diameter of the left ventricle, in order to calculate fractional shortening (FS), wall thickness and stroke volume (SV). After sacrifice hearts were isolated and cut into five equal slices of approximately 2.5 mm thickness. The middle two slices were snap frozen in liquid nitrogen, the apex and the top two slices (as seen from the base of the heart) were embedded in paraffin.

### 2.8. Fluorescence microscopy

The number of fluorescent stem cells in frozen heart slides was determined as previously described by van Dijk et al. (2011), with a minor adaptation that we now used the nuclear stain Hoechst in order to retrace engrafted stem cells. To retrieve Hoechst-positive stem cells and determine putative co-localization with ICAM-1 in the pilot study, four frozen heart slides per rat were stained with monoclonal antibodies against goat-anti-ICAM-1 (1:100, Abcam, Cambridge, UK) and mouse-anti-α-actinin (1:200, 4 °C overnight, Sigma), followed by incubation with a rabbit-anti-goat-FITC and a donkey-anti-mouse Cy5 secondary antibody (both 1:100, BD) for 30 min in the dark.

In the functional study Hoechst-positive cells were also checked for putative differentiation towards cardiomyocytes. For this, four frozen heart slides per rat were counterstained with mouse monoclonal antibodies against troponin T (1:25, 4 °C, overnight; AbD Serotec, UK) or connexin 43 (1:1000, 4 °C, overnight; Abcam), both followed by incubation with a goat-anti-mouse-FITC secondary antibody (1:100, BD).

Fluorescence microscopy (Marianas I.I.I.) was performed with a 10× and a 40× objective (Zeiss). Fluorescent images were analyzed using SlideBook software (I.I.I.). Due to the Hoechst labeling of the ASCs no nuclear counterstain could be used for the whole heart tissue. However, the tissue morphology was clear from both autofluorescence as well as from the cardiomyocyte counterstains. The lung and liver were also screened.

### 2.9. Histological staining to determine infarct size

To determine the infarct size a phosphotungstic acid hematoxylin (PTAH) staining was performed as described previously (van Dijk et al., 2009), on four heart slides per rat distal from the suture: two frozen and two paraffin embedded heart slides. Paraffin embedded slides were deparaffinized and dehydrated, whereas frozen slides were fixed for 10 min in 100% acetone. After washing with PBS, the slides were incubated in Bouin at 60 °C for 30 min. After a cooling down period of 15 min and a wash step in water of 10 min, slides were incubated in PTAH at 60 °C for 60 min. After cooling down, slides were dehydrated, washed in xylene and covered. PTAH stains viable cardiomyocytes purple and infarcted cardiomyocytes pink, allowing infarct area measurements on scanned slide (Pannoramic Desk scanner and Pannoramic Viewer 1.15.3 software 3DHistech, Budapest, Hungary). Infarct size was expressed as the percentage of the surface area per whole heart slide, averaged for four cross sections.

### 2.10. Immunohistochemical staining of macrophages

To determine the inflammatory healing process post-AMI, the number and subtype of macrophages were determined by immunohistochemistry on serial paraffin slides. For total numbers of macrophages a mouse-anti-rat CD68 antibody (1:100, RT, 60 min; Serotec) was used after antigen retrieval with 0.1% pepsin (in 0.02 M HCl, 37 °C, 30 min). For the late, pro-healing M2 subtype of macrophages a mouse-anti-rat ED2 antibody (1:200, RT, 60 min; a gift from prof. C.D. Dijkstra, VUmc, Amsterdam, the Netherlands) was used after antigen retrieval with 10 mM sodium citrate buffer, pH 6.0, by boiling the slides in this buffer for 10 min. A secondary antibody Envision-HRP (1:200, 30 min, DakoCytomation, USA) was used. Staining was visualized using Envision-diaminobenzidin (DakoCytomation). Control slides incubated with PBS instead of primary antibody yielded no staining (not shown). CD68 and ED2 positive cells in the infarct area were scored microscopically using a 20× objective (Zeiss, Germany). Infarct area was measured using Pannoramic Viewer.

### 2.11. Statistical analysis

All *in vitro* experiments were performed at least six times. For all *in vivo* data non-parametric Mann–Whitney or Kruskal–Wallis rank sum test was used, followed by Dunn's multiple comparison (GraphPad Prism 6.0). The echocardiographic data at baseline and at day 7 were analyzed for equal variances, and were subsequently taken together to provide a single value for all measurements at baseline and day 7. These values are displayed in the graphs as dotted lines. A p-value smaller than 0.05 was considered to represent a statistically significant difference. Data is described as mean ± standard error of the mean (SEM).

## 3. Results

### 3.1. In vitro characterization of StemBells

Rat SVF cells were isolated from inguinal fat. The percentage of colony forming cells indicative of the percentage of stem cells in the stromal vascular fraction was 11.1 ± 1.8%. After a culture period of six days, ASCs were characterized and showed stem cell morphology with an average cell size of 14.3 ± 0.3 μm (not shown) in accordance with our previous studies (van Dijk et al., 2011; Naaijkens et al., 2012). Dual-targeted microbubbles were successfully assembled showing the presence of both anti-CD90 and anti-ICAM-1 antibodies on the microbubble shell (Fig. 1B). Next, these dual-targeted microbubbles were added to rat ASCs in a 100:1 ratio to form stem cell-microbubble complexes, named “StemBells” (Fig. 1C). ASCs were coated with an average of 32.5 ± 4.2 microbubbles/cell (Fig. 1D). This number was not affected by ultrasound exposure (30.6 ± 3.7 microbubbles/cell).

The procedure to assemble StemBells, using rat ASCs, did not significantly affect cell viability (ASCs 85.7 ± 2.3% viable cells; StB 87.1 ± 1.4% viable cells). Although exposure to ultrasound slightly, but non-significantly decreased cell viability (StB + US 80.0 ± 2.3% viable

cells; $p = 0.09$), as shown in Fig. 2A. In addition, StemBells with or without exposure to ultrasound were similarly capable of attachment to culture plastic (Fig. 2B), with already 60% attachment after 5 min, increasing up to 95% at 20 min. Next, it was studied, using human ASCs, whether StemBells with dual-targeting microbubbles were susceptible to acoustic radiation force in an *in vitro* flow assay. Ultrasound displaced StemBells to the side of the flow channel in the direction of the ultrasonic wave propagation and perpendicular to the direction of flow with a translation speed of 23.2 mm/s orthogonal to the flow (Fig. 2C). ASCs alone were not susceptible to ultrasound (not shown).

To summarize, StemBells were successfully assembled, susceptible to acoustic radiation force, without affecting the number of microbubbles per StemBell, and without affecting cell viability and attachment rate. These *in vitro* results made application of the StemBell technique suitable for first *in vivo* usage.

### 3.2. Intravenously delivered StemBells target to the infarcted myocardium

In a pilot study StemBells were injected intravenously in five rats 7 days after AMI. No shortness of breath was observed and no rats died as a consequence of injecting StemBells. Using fluorescence microscopy on frozen heart slides to retrieve Hoechst-positive cells it was shown that the StemBells were able to extravasate and bind to the myocardium, specifically in the infarct area ($8.4 \pm 3.3$ cells/mm$^2$), co-localizing with ICAM-1 (Fig. 3A). Virtually no cells were found in the non-infarct areas ($0.1 \pm 0.02$ cell/mm$^2$; Fig. 3B).

### 3.3. StemBells have long term beneficial effects on heart function after AMI

Following the pilot study, we determined in a long term functional study whether injection of StemBells 7 days after AMI improved cardiac function at 42 days post-AMI. To determine putative effects on cardiac function 2D-echocardiography was performed prior to AMI, immediately prior to stem cell injection and immediately prior to sacrifice at day 42 post-AMI. Analysis of the fractional shortening (FS), a measurement reflecting left ventricular contractile capacity showed that contractility declined from $50.3 \pm 1.2\%$ at baseline to $34.3 \pm 1.7\%$ on day 7 (both represented by dotted lines, Fig. 4A). The vehicle group displayed a further decline to $27.0 \pm 1.8\%$ on day 42. The ASC group showed minor improvement ($36.5 \pm 3.1\%$ on day 42), and only the StB group showed a significant improvement in FS ($40.5 \pm 3.8\%$ on day 42; $p < 0.01$) compared with the vehicle group. Stroke volume analysis showed similar results (Fig. 4B), with a significant improvement of stroke volume in the StB group ($0.44 \pm 0.03$ ml) as compared with the vehicle group ($0.32 \pm 0.02$ ml; $p < 0.01$), and compared with baseline ($0.32 \pm 0.01$ ml; $p < 0.05$). Subsequently, the left ventricle wall thickness of the non-infarcted posterior wall was determined to study putative post-AMI hypertrophy (Fig. 4C). No changes in wall thickness were observed on day 7 ($0.18 \pm 0.01$ cm) compared with baseline ($0.19 \pm 0.01$ cm; $p = 0.99$). However, in the vehicle group significant thickening of the posterior wall was found on day 42 ($0.24 \pm 0.02$ cm; $p < 0.01$ *vs.* both baseline and day 7), indicative for cardiac remodeling towards hypertrophy. This thickening was also present, but to a lesser degree in the ASC group ($0.22 \pm 0.01$ cm on day 42; $p < 0.01$ *vs.* baseline and day 7). Notable, the posterior wall in the StB group did not show any changes on day 42 compared with baseline and day 7 ($0.19 \pm 0.01$ cm on day 42; $p = 0.99$), and was significantly different from both the vehicle ($p < 0.05$) and ASC group ($p < 0.05$). No changes were observed in the anterior wall where the infarction was induced (data not shown).

Thirty-five days after injection Hoechst-positive cells were still visible and were predominantly found as solitary cells specifically within the infarct area (Fig. 5A). These labeled stem cells were not found in the lungs or liver. A small, non-significant increase in the number of stem cells was found in the infarct area of StB-treated rats ($4.6 \pm 1.1$ cells/mm$^2$) compared with ASC-treated rats ($3.3 \pm 1.0$ cells/mm$^2$, $p = 0.29$), as shown in Fig. 5B. Hardly any cells were found in the non-infarct area (ASCs $0.03 \pm 0.01$; StB $0.13 \pm 0.08$ cells/mm$^2$). All retrieved stem cells showed expression of the cardiomyocyte markers (Naaijkens et al., 2012) Connexin 43 (Fig. 5C, left panel) and Troponin T (Fig. 5C, right panel), with no difference between the ASC and StB group. Albeit that intensity levels of these markers were markedly lower in the retrieved stem cells than in healthy cardiomyocytes.

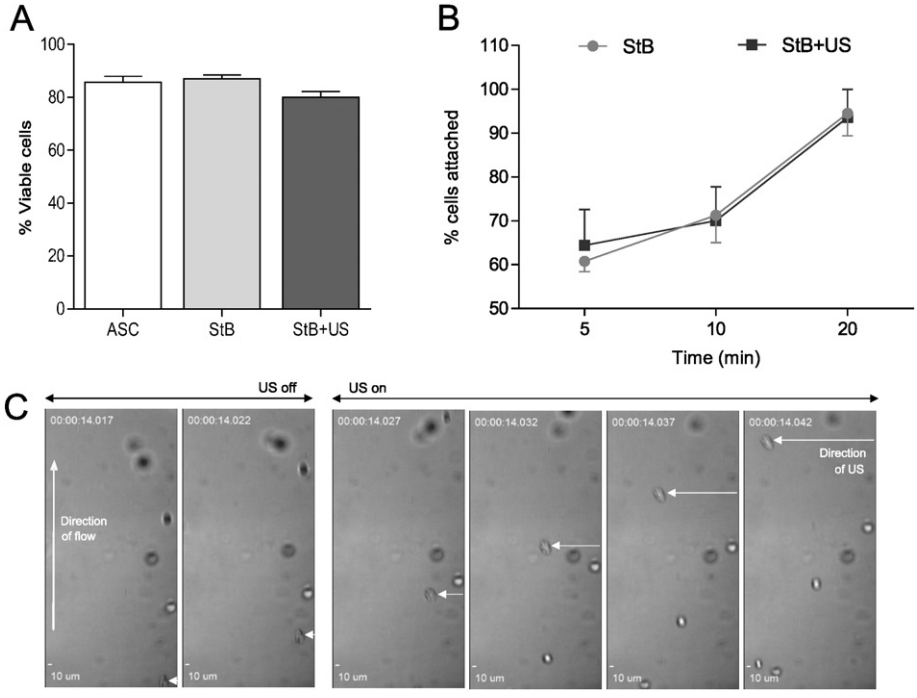


**Fig. 2.** *In vitro* functionality A) Quantification of stem cell viability using flow cytometry with Annexin V and propidium iodide (PI). B) Attachment rate of StemBells with or without ultrasound (US) at 5, 10 and 20 min after seeding to tissue culture plastic. Data is shown as mean ± SEM ($n = 3$). C) Sequential microscopic bright field images demonstrating susceptibly of a StemBell in a flow system. Direction of flow is from bottom to top. Ultrasound exerts acoustic radiation force from right to left. Arrow indicates a StemBell in focus displacing with a translational speed of 23.2 mm/s orthogonal to the flow.

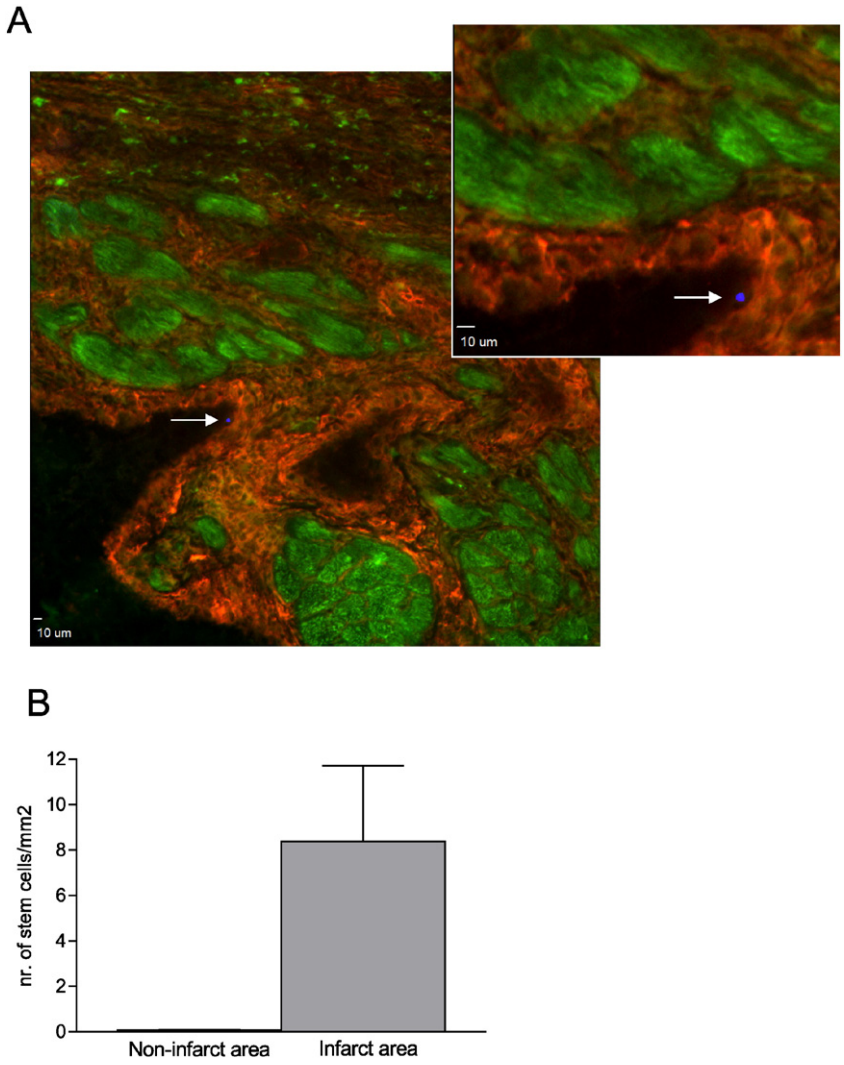


**Fig. 3.** *In vivo* pilot study A) Fluorescence microscopy image showing a Hoechst-positive stem cell (blue) within ICAM-1 positive region (red) next to cardiomyocytes (green). B) Quantification of the number of Hoechst-positive StemBells in non-infarct area and infarct area. Data is shown as mean ± SEM (n = 5).

Next, infarct sizes were determined by a PTAH staining on the heart slides (van Dijk et al., 2011; van Dijk et al., 2009). A small infarct size of 5.9 ± 0.8% was found in the vehicle-treated animals, 5.7 ± 1.2% in ASC-treated animals and 8.0 ± 1.6% in StB-treated animals, with no significant differences between the groups (Fig. 6A; $p = 0.40$).

Finally, the number and subtype of macrophages within the infarct area were quantified to determine a putative effect of the stem cells on the healing process post-AMI. However, also here no differences were found in the total number of macrophages (CD68 positive) per $mm^2$ (Fig. 6B), or the number of pro-healing ED2 positive macrophages (Fig. 6C), nor in the ratio of ED2/CD68 (Fig. 6D).

## 4. Discussion

In this study we described the development of a novel technique to target stem cells specifically to the infarct area by the assembly of stem cell-microbubble complexes, named StemBells. These StemBells were first *in vitro* characterized, showing high viability after assembly and ultrasound exposure, as well as susceptibility to acoustic radiation force. *In vivo* this new stem cell delivery technique proved to be safe for intravenous injection with StemBells reaching the infarct area of the heart. In addition, StemBells significantly improved cardiac function, independent of an effect on infarct size or inflammatory macrophages five weeks after injection.

We developed our novel targeting technique in order to overcome one of the major problems with stem cell therapy, namely the high wash-out of injected stem cells by the blood and low engraftment rate. This high-washout of over 90% by the blood is irrespectively of the delivery route of the stem cells (Hale et al., 2008; Hou et al., 2005; Perin et al., 2008; Baklanov et al., 2006). In the pilot short-term study the retrieved cells co-localized with ICAM-1 positive infarct area three hours after StemBell injection. This demonstrated safe passage of the StemBells through the pulmonary microcirculation and extravasation within the infarct area, without any complications such as shortness of breath or suffocation. Although intravenous delivery has been put away as non-effective due to pulmonary first-pass effect, recent animal studies demonstrated that stem cells do safely traverse the pulmonary circulation in mice (Geng et al., 2014), rats (Zanetti et al., 2015) and pigs (Makela et al., 2015). In addition, we previously demonstrated that culturing ASCs for several passages does result in obstruction in the lungs (van Dijk et al., 2011), indicating that culturing changes the stem cells in such a way that they are entrapped in the lungs. Whereas coupling microbubbles to ASCs which were cultured for only one passage did not lead to entrapment in the lungs. Naturally, smaller cells or cell-constructs traverse the pulmonary circulation easier and faster

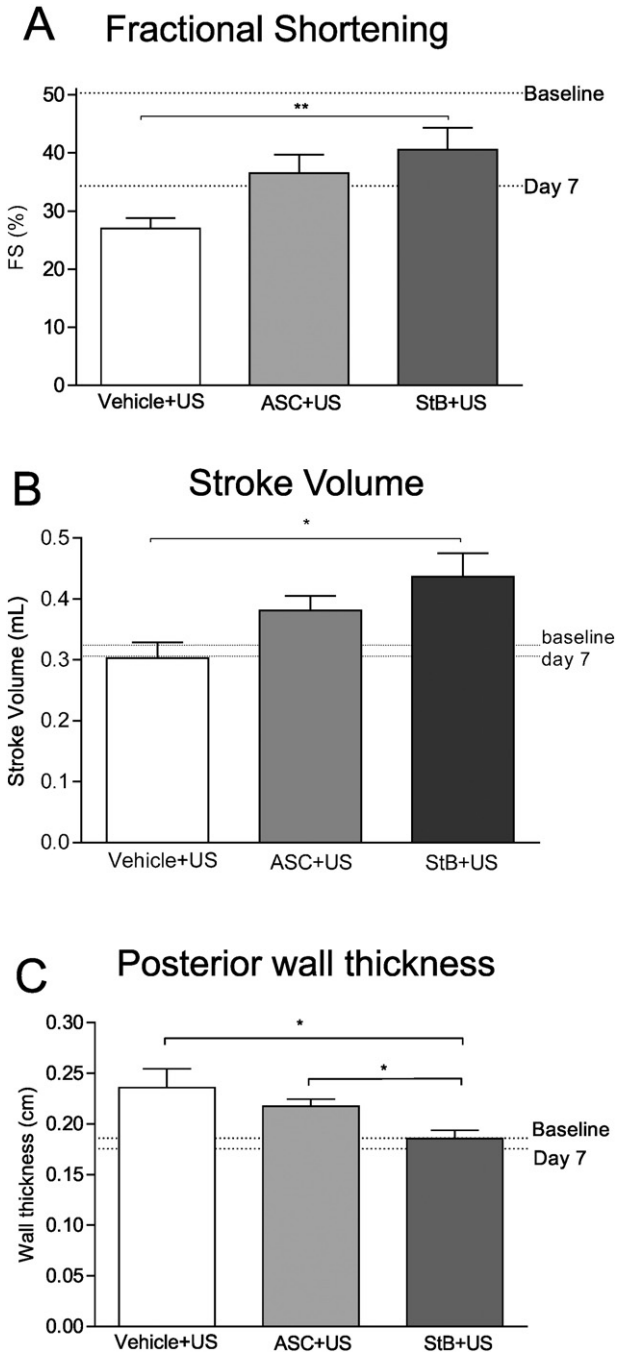


**Fig. 4.** *In vivo* functional data Analysis of echocardiography short-axis images for A) fractional shortening (%) on day 42, with dotted lines representing baseline (day 0) and day 7 post-AMI. B) Stroke volume (ml). C) Posterior wall thickness (cm). Data is shown as mean ± SEM (n = 7 for Vehicle, n = 11 for ASCs, n = 9 for StB).

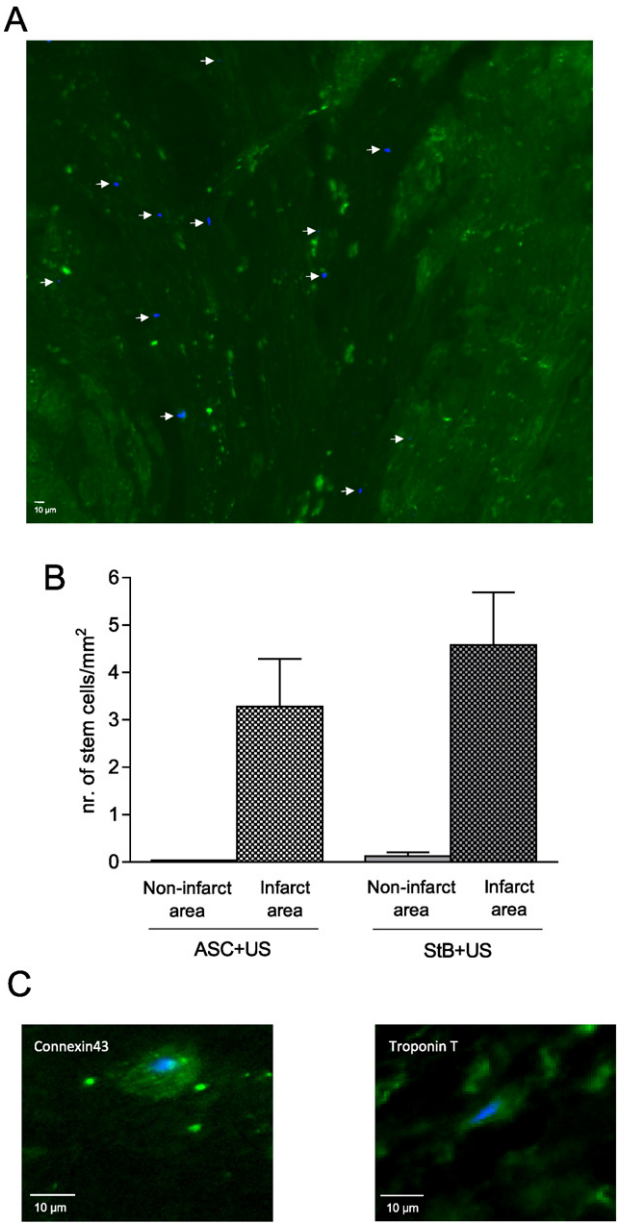


**Fig. 5.** *In vivo* stem cell retrieval A) Fluorescence microscopy image of Connexin 43 (green) stained heart slide. Arrows indicate presence of Hoechst-positive stem cells (blue) within the infarct area. B) Quantification of the number of stem cells per $mm^2$. C) Retrieved stem cells at day 42 stained positive for cardiomyocyte specific markers Connexin 43 (left panel) and Troponin-T (right panel). Data is shown as mean ± SEM (n = 3).

than larger particles and cells (Zanetti et al., 2015). With future clinical application in mind, we deliberately chose for intravenous delivery. For the patient a minimally invasive, intravenous drop with a StemBell suspension at the out-patient clinic is more attractive than an additional catheterization for intracardiac delivery, from both patient and economical view. The patient could even receive multiple treatments of StemBells in combination with ultrasound exposure, something that one would not readily do for intracardiac delivery.

Previously it was described that bi-directional antibodies against myosin light chain in mice (Lee et al., 2007) or VCAM in rats (Lum et al., 2004) that were used to increase homing of hematopoietic stem cells to the heart. The results from our pilot study now demonstrated that our ICAM-1 targeted StemBells had the same effect as the retrieved stem cells co-localized with ICAM-1 upregulated in the infarct area. Even more, StemBells — in addition to their targeting moiety — are susceptible to ultrasound. This was demonstrated by the ability of ultrasound to displace StemBells over a relevant distance *in vitro* in this study, as well as previously in a vitelline vein of a chick embryo (Kokhuis et al., 2014), locally aiding the StemBells to slow down in the bloodstream and enhance contact to the vessel wall. The application of microbubbles in the aid of improving stem cell delivery over the endothelium has been studied before (Ghanem et al., 2009; Toma et al., 2011). In the study performed by Ghanem et al. (2009) ultrasound-mediated microbubble destruction was applied in rats four days post ischemia–reperfusion, and 15 min prior to intra-aortic bone-marrow mesenchymal stem cell (BM-MSC) injection. One hour after injection it was shown that destruction of microbubbles, focused at the infarct site, resulted in significantly enhanced regional adhesion and

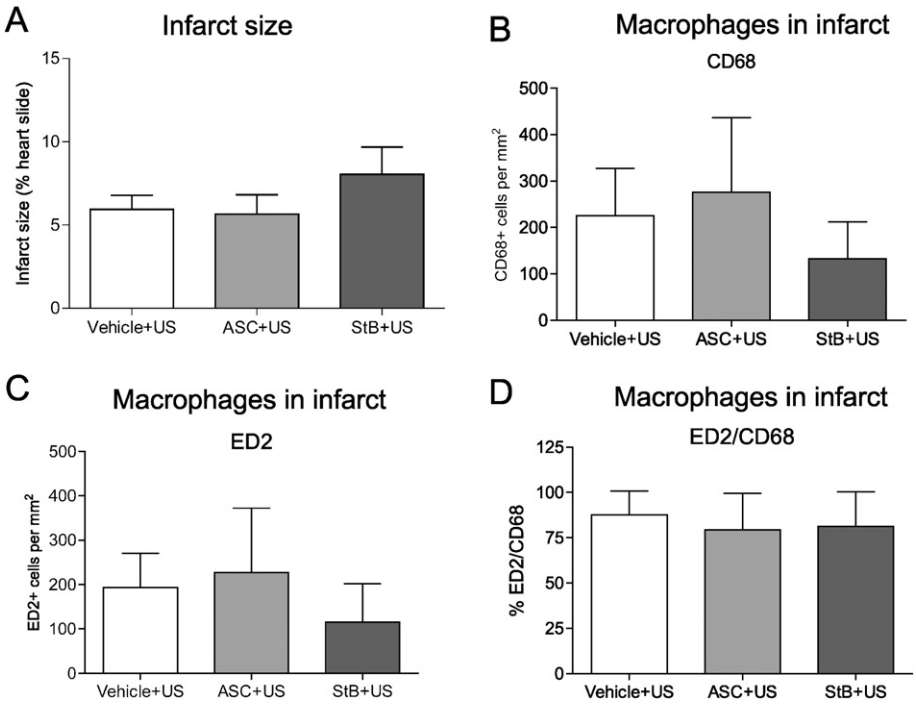


**Fig. 6.** *In vivo* analysis on the long term. A) Quantification of PTAH staining of heart slides showing infarct size. B) Quantification of the number of macrophages: Total number of CD68 positive cells per mm$^2$. C) Number of ED2 positive, type 2 macrophages per mm$^2$. D) ED2 positive cells expressed as percentage of total number of macrophages. Data is shown as mean ± SEM.

transendothelial migration BM-MSCs: 14.6 cells/heart slide *vs.* 9.5 cells/heart slide in animals not pretreated with US and microbubbles (Ghanem et al., 2009). The other study, performed by Toma et al. (2011), showed that non-targeted microbubbles in combination with ultrasound were able to direct BM-MSC to mechanically injured endothelium of a rabbit aorta *in vivo*, resulting in 3.3 cells/mm$^2$ at the ultrasound-exposed segments of the aorta (Toma et al., 2011). Although different experimental models, the number of stem cells we retrieved was in the same order of magnitude: 8.4 cells/mm$^2$ (13.4 cells/heart slide) in the infarct area three hours after injection.

Following the safety pilot study, a long term functional study was performed where treatment of the rats with StemBells significantly improved their cardiac function as demonstrated by echocardiography. A functional improvement was found in a significantly better fractional shortening in the StemBell group, concordantly, the StemBell group had the highest stroke volume. Finally in the StemBell group thickening of the non-infarcted posterior left ventricle wall was prevented. These functional effects could not be explained by a difference in infarct size between the groups. In the literature several studies have shown improved cardiac function without an effect on infarct size, *e.g.* in rats where ASCs were injected 24 h (Danoviz et al., 2010) or 1 week(Rasmussen et al., 2014) post-infarction in a model with a permanent ligation, as well as in pigs where ASCs were injected 1 week post-infarction induced by a balloon angioplasty for 3 h followed by reperfusion (Valina et al., 2007). Besides studying infarct size, we also analyzed other mechanisms that might explain the improved cardiac function by StemBells, such as cardiac differentiation or an effect on inflammatory cells. We did find cardiomyocyte specific markers Connexin 43 and Troponin-T on the retraced stem cells, which may be indicative for partial differentiation towards cardiomyocytes (Naaijkens et al., 2012; Bai et al., 2010). However, the low number of retrieved stem cells makes it highly unlikely that differentiation is a key mechanism.

Recently it was described that the ratio between the early and late subtype of macrophages provides information about the course of infarct repair, especially as macrophages in the infarct area can release substances that are of influence on the non-infarct healthy cardiomyocytes (Ben-Mordechai et al., 2013; Cho et al., 2014). Therefore, we analyzed macrophage subpopulations within the infarct area by ED2, the sole marker for rat type 2 anti-inflammatory macrophages identified. It was observed, that only very focally macrophages were present in the non-infarct area in all groups. However, no difference between the groups was found for the type 2 macrophages within the infarct area.

The fact that we found only a small difference in the number of retrieved stem cells five weeks after injection may indicate that the mechanism behind improved heart function might be explained by substances produced by StemBells exposed to ultrasound directly after injection, but not by stem cells exposed to ultrasound. It has been demonstrated that BM-MSCs produce and secrete a wide range of cytokines, chemokines and growth factors (extensively reviewed by Gnecchi et al., 2008), and that hypoxia, *e.g.* the infarct area, increases this production and secretion (Kinnaird et al., 2004; Gnecchi et al., 2008). According to Gnecchi et al. (2008) some of the paracrine factors released may alter the extracellular matrix, resulting in more favorable post-infarction remodeling and strengthening of the infarct scar (Gnecchi et al., 2008). In addition, there is data suggesting that factors secreted by stem cells may positively influence cardiac contractility. For example, insulin-like growth factor (IGF-1) improved myocardial function in both normal and infarcted adult rat hearts (Cittadini et al., 1996). Another suggestion is the positive effect of secreted substances on bioenergetics in the post-infarcted heart. Feygin et al. (2007) demonstrated in pigs that hearts in the AMI group developed severe contractile dyskinesis in the infarct and border zone, whereas BM-MSC transplantation significantly improved contractile performance. Interestingly, they also did not find an effect on infarct size. Because of low cell engraftment, the authors concluded that the observed beneficial effects were most likely attributable to paracrine repair mechanisms (Feygin et al., 2007). It is also known that an infarction results in a decrease in cardiomyocyte contractility outside of the infarct area (Loennechen et al., 2002). It can be speculated that the paracrine effects of StemBells exposed to ultrasound may positively affect cardiac contractility in the remote areas, thereby preventing cardiac remodeling, and improving fractional shortening, although further research in necessary to confirm this.

The results described here demonstrate the potential of this novel targeting technique. Although we focused on cardiac repair in AMI, the StemBell technique bears the perspective to be applicable in a variety of diseases that may require regenerative cellular therapy.

In conclusion, the StemBell technique is a novel and feasible technique, able to improve cardiac function post-AMI in rats.

## Funding

This work was supported by a grant from the Dutch Technology Foundation STW (project 10507).

## Disclosures

None.

## Acknowledgments

We acknowledge the kind gift of the ED2 antibody by prof. C.D. Dijkstra (Department of Molecular and Cellular Biology and Immunology, VU University Medical Center, Amsterdam, the Netherlands).

## References

Assmus, B., Leistner, D.M., Schachinger, V., Erbs, S., Elsasser, A., Haberbosch, W., Hambrecht, R., Sedding, D., Yu, J., Corti, R., Mathey, D.G., Barth, C., Mayer-Wehrstein, C., Burck, I., Sueselbeck, T., Dill, T., Hamm, C.W., Tonn, T., Dimmeler, S., Zeiher, A.M., 2014. Long-term clinical outcome after intracoronary application of bone marrow-derived mononuclear cells for acute myocardial infarction: migratory capacity of administered cells determines event-free survival. Eur. Heart J. 35 (19), 1275–1283.

Bai, X., Yan, Y., Song, Y.H., Seidensticker, M., Rabinovich, B., Metzele, R., Bankson, J.A., Vykoukal, D., Alt, E., 2010. Both cultured and freshly isolated adipose tissue-derived stem cells enhance cardiac function after acute myocardial infarction. Eur. Heart J. 31 (4), 489–501.

Baklanov, D.V., Moodie, K.M., McCarthy, F.E., Mandrusov, E., Chiu, J., Aswonge, G., Cheng, J., Chow, M., Simons, M., de Muinck, E.D., 2006. Comparison of transendocardial and retrograde coronary venous intramyocardial catheter delivery systems in healthy and infarcted pigs. Catheter. Cardiovasc. Interv. 68 (3), 416–423.

Ben-Mordechai, T., Holbova, R., Landa-Rouben, N., Harel-Adar, T., Feinberg, M.S., Elrahman, I.A., Blum, G., Epstein, F., Silman, Z., Cohen, S., Leor, J., 2013. Macrophage subpopulations are essential for infarct repair with and without stem cell therapy. J. Am. Coll. Cardiol. 62 (20), 1890–1901.

Benson, V., McMahon, A.C., Lowe, H.C., 2007. ICAM-1 in acute myocardial infarction: a potential therapeutic target. Curr. Mol. Med. 7 (2), 219–227.

Berardi, G.R., Rebelatto, C.K., Tavares, H.F., Ingberman, M., Shigunov, P., Barchiki, F., Aguiar, A.M., Miyague, N.I., Francisco, J.C., Correa, A., Senegaglia, A.C., Suss, P.H., Moutinho, J.A., Sotomaior, V.S., Nakao, L.S., Brofman, P.S., 2011. Transplantation of SNAP-treated adipose tissue-derived stem cells improves cardiac function and induces neovascularization after myocardium infarct in rats. Exp. Mol. Pathol. 90 (2), 149–156.

Carvalho, P.H., Daibert, A.P., Monteiro, B.S., Okano, B.S., Carvalho, J.L., Cunha, D.N., Favarato, L.S., Pereira, V.G., Augusto, L.E., Del Carlo, R.J., 2013. Differentiation of adipose tissue-derived mesenchymal stem cells into cardiomyocytes. Arq. Bras. Cardiol. 100 (1), 82–89.

Cho, D.I., Kim, M.R., Jeong, H.Y., Jeong, H.C., Jeong, M.H., Yoon, S.H., Kim, Y.S., Ahn, Y., 2014. Mesenchymal stem cells reciprocally regulate the M1/M2 balance in mouse bone marrow-derived macrophages. Exp. Mol. Med. 46, e70.

Cittadini, A., Stromer, H., Katz, S.E., Clark, R., Moses, A.C., Morgan, J.P., Douglas, P.S., 1996. Differential cardiac effects of growth hormone and insulin-like growth factor-1 in the rat. A combined in vivo and in vitro evaluation. Circulation 93 (4), 800–809.

Danoviz, M.E., Nakamuta, J.S., Marques, F.L., SL, dos, EC, Alvarenga, AA, dos Santos, EL, Antonio, IT, Schettert, PJ, Tucci, JE, Krieger, 2010. Rat adipose tissue-derived stem cells transplantation attenuates cardiac dysfunction post infarction and biopolymers enhance cell retention. PLoS One 5 (8), e12077.

Dijkmans, P.A., Juffermans, L.J.M., Musters, R.J.P., van Wamel, A., ten Cate, F., van Gilst, W., Visser, C.A., de Jong, N., Kamp, O., 2004. Microbubbles and ultrasound: from diagnosis to therapy. Eur. J. Echocardiogr. 5 (4), 245–256.

Feygin, J., Mansoor, A., Eckman, P., Swingen, C., Zhang, J., 2007. Functional and bioenergetic modulations in the infarct border zone following autologous mesenchymal stem cell transplantation. Am. J. Physiol. Heart Circ. Physiol. 293 (3), H1772–H1780.

Geng, Y., Zhang, L., Fu, B., Zhang, J., Hong, Q., Hu, J., Li, D., Luo, C., Cui, S., Zhu, F., Chen, X., 2014. Mesenchymal stem cells ameliorate rhabdomyolysis-induced acute kidney injury via the activation of M2 macrophages. Stem Cell Res. Ther. 5 (3), 80.

Ghanem, A., Steingen, C., Brenig, F., Funcke, F., Bai, Z.Y., Hall, C., Chin, C.T., Nickenig, G., Bloch, W., Tiemann, K., 2009. Focused ultrasound-induced stimulation of microbubbles augments site-targeted engraftment of mesenchymal stem cells after acute myocardial infarction. J. Mol. Cell. Cardiol. 47 (3), 411–418.

Gnecchi, M., Zhang, Z., Ni, A., Dzau, V.J., 2008. Paracrine mechanisms in adult stem cell signaling and therapy. Circ. Res. 103 (11), 1204–1219.

Hale, S.L., Dai, W., Dow, J.S., Kloner, R.A., 2008. Mesenchymal stem cell administration at coronary artery reperfusion in the rat by two delivery routes: a quantitative assessment. Life Sci. 83 (13–14), 511–515.

Hou, D., Youssef, E.A., Brinton, T.J., Zhang, P., Rogers, P., Price, E.T., Yeung, A.C., Johnstone, B.H., Yock, P.G., March, K.L., 2005. Radiolabeled cell distribution after intramyocardial, intracoronary, and interstitial retrograde coronary venous delivery: implications for current clinical trials. Circulation 112 (9 Suppl), I150–I156.

Houtgraaf, J.H., den Dekker, W.K., van Dalen, B.M., Springeling, T., JR, de, RJ, van Geuns, ML, Geleijnse, Fernandez-Aviles, F., Zijlsta, F., PW, Serruys, HJ, Duckers, 2012. First experience in humans using adipose tissue-derived regenerative cells in the treatment of patients with ST-segment elevation myocardial infarction. J. Am. Coll. Cardiol. 59 (5), 539–540.

Janssens, S., Dubois, C., Bogaert, J., Theunissen, K., Deroose, C., Desmet, W., Kalantzi, M., Herbots, L., Sinnaeve, P., Dens, J., Maertens, J., Rademakers, F., Dymarkowski, S., Gheysens, O., Van, C.J., Bormans, G., Nuyts, J., Belmans, A., Mortelmans, L., Boogaerts, M., Van de Werf, F., 2006. Autologous bone marrow-derived stem-cell transfer in patients with ST-segment elevation myocardial infarction: double-blind, randomised controlled trial. Lancet 367 (9505), 113–121.

Jeevanantham, V., Butler, M., Saad, A., Abdel-Latif, A., Zuba-Surma, E.K., Dawn, B., 2012. Adult bone marrow cell therapy improves survival and induces long-term improvement in cardiac parameters: a systematic review and meta-analysis. Circulation 126 (5), 551–568.

Kinnaird, T., Stabile, E., Burnett, M.S., Shou, M., Lee, C.W., Barr, S., Fuchs, S., Epstein, S.E., 2004. Local delivery of marrow-derived stromal cells augments collateral perfusion through paracrine mechanisms. Circulation 109 (12), 1543–1549.

Klibanov, A.L., Rasche, P.T., Hughes, M.S., Wojdyla, J.K., Galen, K.P., Wible Jr., J.H., Brandenburger, G.H., 2004. Detection of individual microbubbles of ultrasound contrast agents: imaging of free-floating and targeted bubbles. Investig. Radiol. 39 (3), 187–195.

Kokhuis, T.J., Garbin, V., Kooiman, K., Naaijkens, B.A., Juffermans, L.J., Kamp, O., van der Steen, A.F., Versluis, M., JN, de, 2013. Secondary Bjerknes forces deform targeted microbubbles. Ultrasound Med. Biol. 39 (3), 490–506.

Kokhuis, T.J., Skachkov, I., Naaijkens, B.A., Juffermans, L.J., Kamp, O., Kooiman, K., van der Steen, A.F., Versluis, M., JN, de, 2014. Intravital microscopy of localized stem cell delivery using microbubbles and acoustic radiation force. Biotechnol. Bioeng. 112 (1), 220–227.

Lee, R.J., Fang, Q., Davol, P.A., Gu, Y., Sievers, R.E., Grabert, R.C., Gall, J.M., Tsang, E., Yee, M.S., Fok, H., Huang, N.F., Padbury, J.F., Larrick, J.W., Lum, L.G., 2007. Antibody targeting of stem cells to infarcted myocardium. Stem Cells 25 (3), 712–717.

Loennechen, J.P., Wisloff, U., Falck, G., Ellingsen, O., 2002. Cardiomyocyte contractility and calcium handling partially recover after early deterioration during post-infarction failure in rat. Acta Physiol. Scand. 176 (1), 17–26.

Lum, L.G., Fok, H., Sievers, R., Abedi, M., Quesenberry, P.J., Lee, R.J., 2004. Targeting of Lin-Sca + hematopoietic stem cells with bispecific antibodies to injured myocardium. Blood Cells Mol. Dis. 32 (1), 82–87.

Makela, T., Takalo, R., Arvola, O., Haapanen, H., Yannopoulos, F., Blanco, R., Ahvenjarvi, L., Kiviluoma, K., Kerkela, E., Nystedt, J., Juvonen, T., Lehenkari, P., 2015. Safety and biodistribution study of bone marrow-derived mesenchymal stromal cells and mononuclear cells and the impact of the administration route in an intact porcine model. Cytotherapy 17 (4), 392–402.

Naaijkens, B.A., Niessen, H.W., Prins, H.J., Krijnen, P.A., Kokhuis, T.J., JN, de, VW, van Hinsbergh, Kamp, O., MN, Helder, RJ, Musters, DA, van, LJ, Juffermans, 2012. Human platelet lysate as a fetal bovine serum substitute improves human adipose-derived stromal cell culture for future cardiac repair applications. Cell Tissue Res. 348 (1), 119–130.

Oedayrajsingh-Varma, M.J., van Ham, S.M., Knippenberg, M., Helder, M.N., Klein-Nulend, J., Schouten, T.E., Ritt, M.J., van Milligen, F.J., 2006. Adipose tissue-derived mesenchymal stem cell yield and growth characteristics are affected by the tissue-harvesting procedure. Cytotherapy 8 (2), 166–177.

Perin, E.C., Silva, G.V., Assad, J.A., Vela, D., Buja, L.M., Sousa, A.L., Litovsky, S., Lin, J., Vaughn, W.K., Coulter, S., Fernandes, M.R., Willerson, J.T., 2008. Comparison of intracoronary and transendocardial delivery of allogeneic mesenchymal cells in a canine model of acute myocardial infarction. J. Mol. Cell. Cardiol. 44 (3), 486–495.

Pfeffer, M.A., Pfeffer, J.M., Fishbein, M.C., Fletcher, P.J., Spadaro, J., Kloner, R.A., Braunwald, E., 1979. Myocardial infarct size and ventricular function in rats. Circ. Res. 44 (4), 503–512.

Rangappa, S., Fen, C., Lee, E.H., Bongso, A., Sim, E.K., 2003. Transformation of adult mesenchymal stem cells isolated from the fatty tissue into cardiomyocytes. Ann. Thorac. Surg. 75 (3), 775–779.

Rasmussen, J.G., Frobert, O., Holst-Hansen, C., Kastrup, J., Baandrup, U., Zachar, V., Fink, T., Simonsen, U., 2014. Comparison of human adipose-derived stem cells and bone marrow-derived stem cells in a myocardial infarction model. Cell Transplant. 23 (2), 195–206.

Shah, V.K., Shalia, K.K., 2011. Stem cell therapy in acute myocardial infarction: a pot of gold or Pandora's box. Stem Cells Int. 536758.

Toma, C., Fisher, A., Wang, J., Chen, X., Grata, M., Winston, B., Leeman, J., Kaya, M., Fu, H., Lavery, L., Fischer, D., Wagner, W., Villanueva, F.S., 2011. Vascular endoluminal delivery of stem cells using acoustic radiation force. Tissue Eng. A 17 (9–10), 1457–1464.

Valina, C., Pinkernell, K., Song, Y.H., Bai, X., Sadat, S., Campeau, R.J., Le Jemtel, T.H., Alt, E., 2007. Intracoronary administration of autologous adipose tissue-derived stem cells improves left ventricular function, perfusion, and remodelling after acute myocardial infarction. Eur. Heart J. 28 (21), 2667–2677.

van Dijk, A., Niessen, H.W., Zandieh, D.B., Visser, F.C., van Milligen, F.J., 2008. Differentiation of human adipose-derived stem cells towards cardiomyocytes is facilitated by laminin. Cell Tissue Res. 334 (3), 457–467.

van Dijk, A., Krijnen, P.A., Vermond, R.A., Pronk, A., Spreeuwenberg, M., Visser, F.C., Berney, R., Paulus, W.J., Hack, C.E., van Milligen, F.J., Niessen, H.W., 2009. Inhibition of type 2A secretory phospholipase A2 reduces death of cardiomyocytes in acute myocardial infarction. Apoptosis 14 (6), 753–763.

van Dijk, A., Naaijkens, B.A., Jurgens, W.J., Nalliah, K., Sairras, S., van der Pijl, R.J., Vo, K., Vonk, A.B., van Rossum, A.C., Paulus, W.J., van Milligen, F.J., Niessen, H.W., 2011. Reduction of infarct size by intravenous injection of uncultured adipose derived stromal cells in a rat model is dependent on the time point of application. Stem Cell Res. 7 (3), 219–229.

Wollert, K.C., Meyer, G.P., Lotz, J., Ringes-Lichtenberg, S., Lippolt, P., Breidenbach, C., Fichtner, S., Korte, T., Hornig, B., Messinger, D., Arseniev, L., Hertenstein, B., Ganser, A., Drexler, H., 2004. Intracoronary autologous bone-marrow cell transfer after myocardial infarction: the BOOST randomised controlled clinical trial. Lancet 364 (9429), 141–148.

Yamada, Y., Wang, X.D., Yokoyama, S., Fukuda, N., Takakura, N., 2006. Cardiac progenitor cells in brown adipose tissue repaired damaged myocardium. Biochem. Biophys. Res. Commun. 342 (2), 662–670.

Zanetti, A., Grata, M., Etling, E.B., Panday, R., Villanueva, F.S., Toma, C., 2015. Suspension-expansion of bone marrow results in small mesenchymal stem cells exhibiting increased transpulmonary passage following intravenous administration. Tissue Eng. Part C Methods 21 (7), 683–692.